J Mater Sci (2011) 46:4562–4567
DOI 10.1007/s10853-011-5354-6

Phase transition and mechanical properties of constraint-aged Ni–Mn–Ga–Ti magnetic shape memory alloy

G. F. Dong · Z. Y. Gao · X. L. Zhang · W. Cai · J. H. Sui

Received: 22 June 2010 / Accepted: 31 January 2011 / Published online: 19 February 2011

Abstract Ni–Mn–Ga Heusler-type ferromagnetic shape memory alloys are attractive materials for micro-actuator, but the relatively poor ductility and low strength of Ni–Mn–Ga alloys have triggered a great deal of interest. In this study, we attempt to introduce some ductile second phase in the alloy by partially substituting Ti for Ga and constraint aging treatment. The results show that the martensitic transformation temperature first decreases and then increases slightly with the increasing of constraint-aging temperature, which can be attributed to the decrease of Ni content in the matrix and strengthening effect of the second particles. It is found that the amount of the Ni-rich precipitates by constraint-aged samples is more and the size of the second phase particle is smaller than that of the free-aged samples. The compressive stress and ductility can be significantly improved by the constraint-aging treatment, and the maximum compressive stress for constraint-aging alloy is about 1400 MPa, which is the highest value up to date compared with the 400 MPa in solution-treated Ni–Mn–Ga–Ti alloy and about 900 MPa in Ni–Mn–Ga–Ti alloy free-aged at 1073 K for 3 h. Scanning electron microscopy observations of fracture surfaces confirm that the Ni-rich second phase play a key role in improving the compression stress and ductility of Ni–Mn–Ga–Ti alloy.

G. F. Dong (✉) · X. L. Zhang
Department of Physics, Dalian University, Dalian 116622, China
e-mail: dgfu0451@sina.com

G. F. Dong
College of Physics and Optoelectronic Engineering, Dalian University of Technology, Dalian 116024, China

Z. Y. Gao · W. Cai · J. H. Sui
National Key Laboratory Precision Hot Processing of Metals, School of Materials Science and Engineering, Harbin Institute of Technology, P. O. Box 405, Harbin 150001, China

Introduction

Ni–Mn–Ga alloy has been regarded as one of the most promising candidates to be actuator materials due to their large magnetic-field-induced strain (MFIS) and high response frequency, resulting from the magnetically controlled twin boundary movement [1–4]. Up to date, the large MFIS is observed in certain ferromagnetic martensite of these alloys, for example, very large MFISs of 6% in tetragonal 5 M martensite and about 10% in 7 M martensite [5, 6]. However, practical application of Ni–Mn–Ga alloys is limited to its extreme brittleness and low strength. Improving mechanical property has become a priority in the development of Ni–Mn–Ga alloys.

In order to improve the mechanical properties, there has been growing interest in the modification of Ni–Mn–Ga alloys by adding the fourth elements. Recently, several rare earth elements [7–12], Fe [13], Cu [14], and Co [15, 16] have been added to ternary Ni–Mn–Ga alloys. It was found that the bending strength of Ni–Mn–Ga alloys was increased by adding earth elements Gd, Tb, or Sm. Tsuchiya et.al [9] also reported that the addition of Nd significantly improved the compressive ductility of the alloy. Recently, Titanium element has been added to ternary Ni–Mn–Ga alloys to form a ductile Ni_3Ti second phase, and a significant improvement in the compressive strength and ductility of the aged Ni–Mn–Ga–Ti alloys have been reported [17–20]. It was found that the mechanical behavior of Ni–Mn–Ga alloy could be remarkably increased by forming small amounts of Ni_3Ti second phase through Ti doping and aging treatment, as occurs in Ni–Co–Al and Ni–Al shape

memory alloy. Also, the highest compressive strength of 1403 Mpa is obtained in alloy constant-strain aged at 873 K for 3 h; this is about 500 MPa higher than that of the conventional aging alloy [18]. In this study, we continue to investigate the influence of the constraint aging under constant strain on the phase transition and mechanical properties of quaternary $Ni_{53}Mn_{23.5}Ga_{18.5}Ti_5$ alloy and their relation to microstructural changes.

Experimental

An ingot of $Ni_{53}Mn_{23.5}Ga_{18.5}Ti_5$ alloys was prepared from high purity elements by melting four times in an arc-melting furnace under an argon atmosphere to ensure the homogenization, and then casted into a chilled copper mold to obtain a rod with a dimension of 10 mm in diameter and 70 mm in length. The rod was sealed in a quartz tube with a vacuum of 10^{-4} Torr and annealed at 1273 K for 5 h followed by quenching into ice-water to achieve the high chemical order. Cylindrical samples with a dimension of $\Phi 3 \times 5$ mm for compression testing were cut from the ingot, and were subjected to 2% compression deformation for constraint aging at various temperatures for 3 h in an argon atmosphere, followed by water quenching.

The phase transformation temperatures are measured by a Perkin-Elmer diamond differential scanning calorimetry (DSC) for a temperature range of 100–400 K with the 20 K/min heating and cooling rate. X-ray diffraction (XRD) measurements were performed as a means of crystal structure determination using a Rigaku D/max-rB with Cu K_α radiation. Microstructure observations were made with a MX2600FE scanning electron microscopy (SEM) equipped with an X-ray energy dispersive spectroscopy (EDS) analysis system and a Philips CM-12 transmission electron microscopy (TEM) operated at 120 kV. TEM specimens were electrochemically polished using an electrolyte of 10% perchloric acid and 90% ethanol at 253 K. The compress tests were preformed at ambient temperature on an Instron-5569 test system at a crosshead displacement speed of 0.05 mm/min.

Results and discussion

Figure 1a illustrates the DSC curves of the solution-treated and constraint-aged $Ni_{53}Mn_{23.5}Ga_{18.5}Ti_5$ alloy. It can be seen that there is only one endothermic or one exothermic peak in the heating or cooling curves, respectively, characterizing the typical one-step thermoelastic martensitic transformation. The martensitic transformation temperatures determined by the tangle method from the DSC curves, and the transformation temperatures as a function of aging temperature is presented in the Fig. 1b. Significantly, with increasing aging temperature, the transformation temperatures decrease first and then increase slightly.

The effect of the constraint-aging on the transformation behavior can be explained in terms of two factors, the composition of the matrix and the coherency of the second particles. According to the previous investigations [21–23], the martensitic transformation temperatures of Ni–Mn–Ga alloys are strongly related to the electron concentration (e/a). With increasing aging time, the amount and the size of the Ni-rich second phases increase, so the content of Ni in the matrix decreases, causing the decrease of electron concentration. Therefore, the composition change of the matrix cause the transformation temperature to decrease until the composition of the matrix approaches the equilibrium one after aging. Moreover, the transformation temperatures are also affected by the microstructure as well as the matrix composition. The fine precipitates strengthen

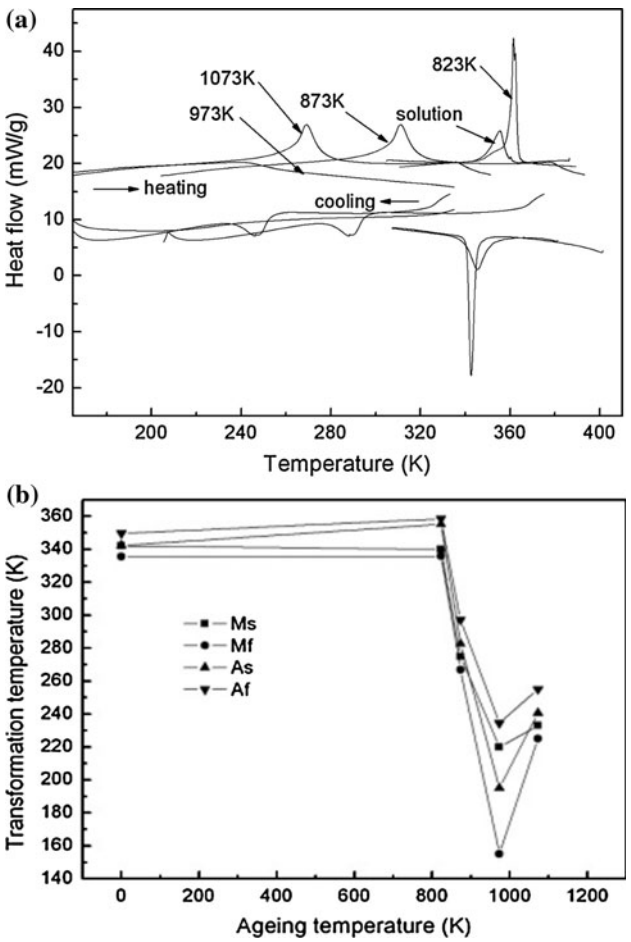

Fig. 1 **a** DSC curves for the $Ni_{53}Mn_{23.5}Ga_{18.5}Ti_5$ alloy constraint-aged at different temperatures for 3 h; **b** the dependence of the martensitic transformation temperature on the constraint-aging temperature

the matrix and thus suppress the shape changes associated with the transformation, resulting in the decrease of transformation temperatures. With the increasing aging temperature, the particles become coarse and lose the coherent interface with matrix, and the strengthening effect is weaker than the fine particle, resulting the increasing of the transformation temperature in the aging temperature range between 973 and 1073 K.

In order to investigate the effect of constraint aging on the mechanical property, compression tests are carried out at room temperature. All the samples are compressed to fracture. Figure 2 presents the compressive stress–strain curves of solution-treated and aging-treated the $Ni_{53}Mn_{23.5}Ga_{18.5}Ti_5$ alloy at room temperature. It should be noted that the deformation for aged samples was mainly due to the dislocation mechanism. It can be also found that good mechanical properties are exhibited in the aging-treatment samples. It is inferred that this is due to the presence of fine coherent second particles in the matrix. Moreover, the constraint-aged alloys exhibit a higher strength over 1400 MPa combined with high ductility over 7.8%.

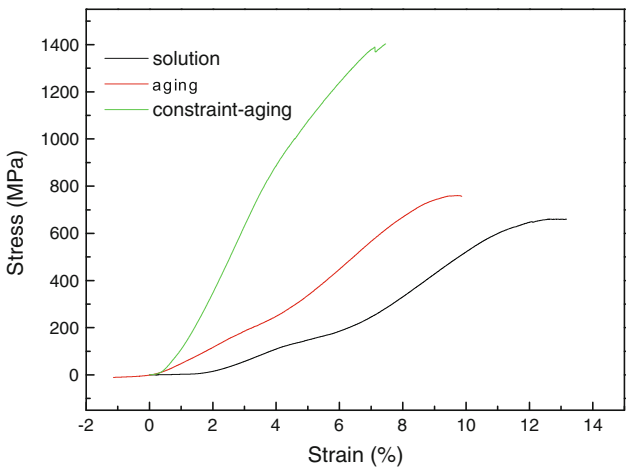

Fig. 2 Strain–stress curves for $Ni_{53}Mn_{23.5}Ga_{18.5}Ti_5$ alloys under various heat-treatment conditions (Color figure online)

Figure 3 shows the dependence of compressive strength and compression strain on the aging temperature for constraint-aged $Ni_{53}Mn_{23.5}Ga_{18.5}Ti_5$ samples. One can seen that the compressive stress increases at first and subsequently decreases while the compressive strain increases with increasing aging temperature. It is noted the maximum compressive strength for constraint-aged sample is obtained in $Ni_{53}Mn_{23.5}Ga_{18.5}Ti_5$ alloy constraint-aged at 873 K for 3 h, and at a nearly 1400 MPa is the highest compressive stress up to date compared with the 400 MPa in solution-treated Ni–Mn–Ga–Ti alloy and about 900 MPa in Ni–Mn–Ga–Ti alloy free-aged at 1073 K for 3 h. Moreover, the maximum compressive strain obtained in the sample constraint-aged at 1173 K for 3 h is approximately 12%, which is just slightly lower than that of the solution-treated alloy and the free-aged samples.

Figure 4 shows the SEM images of the $Ni_{53}Mn_{23.5}Ga_{18.5}Ti_5$ alloys after the conventional aging treatment and constant-strain aging treatment, respectively. It can be seen that the microstructure of the aged alloys is characterized by the presence of dispersed particle with an average size of several micrometer. The fine dispersed lenticular-shape second particles are homogeneously precipitated inside the grain while some water-vapor like bubbles can also be observed in the boundary. It also should be noted that the particle size of second phase gets smaller and its amount increases in the constraint-aged sample in comparison with the free-aged sample. Maybe, this offers a simple way of controlling the crystallite size of second phase consistent with the literature [24].

The TEM observations were performed to reveal the evolution of the microstructure during constraint aging, and the results are shown in Fig. 5. After solution treatment at 1273 K for 5 h, $Ni_{53}Mn_{23.5}Ga_{18.5}Ti_5$ shape memory alloy did not show any precipitates [17]. Figure 5 shows the bright-field images for the sample constraint aged at 823, 873, 973, and 1073 K for 3 h under constant 2%

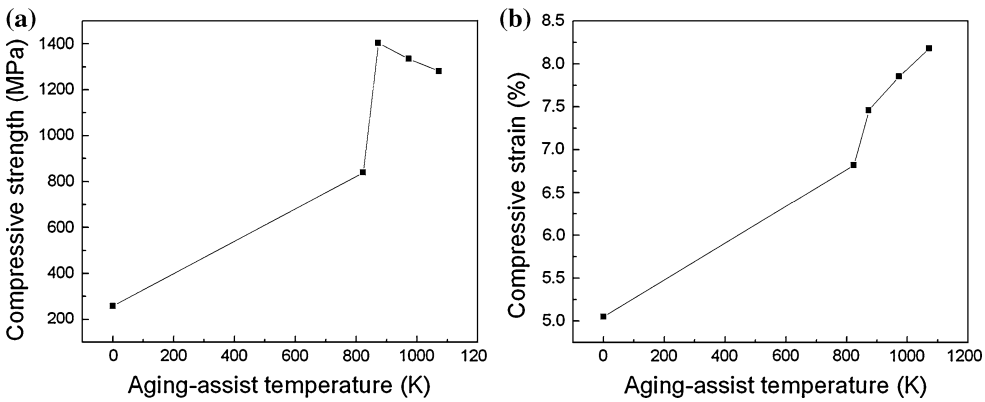

Fig. 3 Effect of aging-assist temperature on the compressive strength and strain of aged-assist $Ni_{53}Mn_{23.5}Ga_{18.5}Ti_5$ alloys

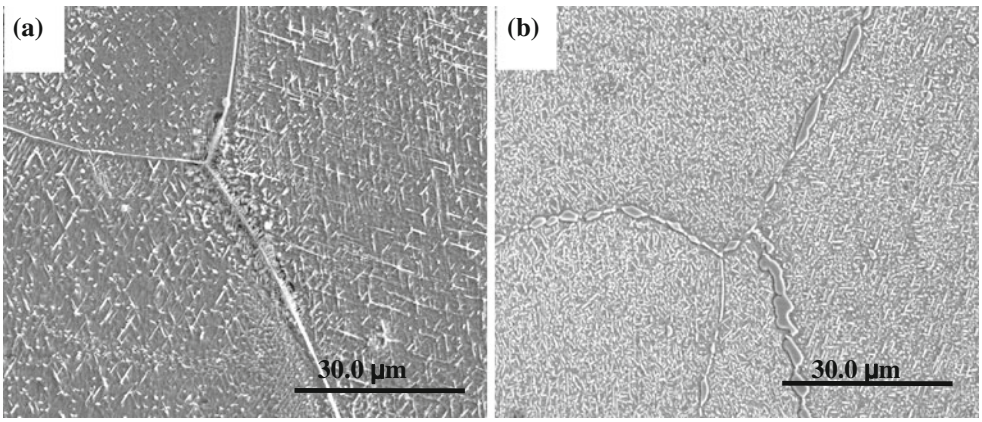

Fig. 4 SEM images of $Ni_{53}Mn_{23.5}Ga_{18.5}Ti_5$ alloys aged at 873 K for 3 h. **a** Without constraint strain, **b** with 2% compression constant strain

compression strain after the solution treatment, respectively. It can be seen that the size of the precipitate increases with the increasing aging temperature. The precipitates were confirmed to be a Ni_3Ti phase by electron diffraction and EDS [17, 18]. The bright-field image also shows the characteristic morphology of the precipitates. That is, the lenticular shape precipitates are observed along two directions. It should also be noted that some dislocations appear (indexed by arrows) when the aging time exceeded 973 K, indicating that the precipitates lose the coherent interface with the matrix.

Since the deformation of the specimens exhibits the characteristics of the dislocation mechanism, the critical stress needed to form a dislocation line through the second particle can be expressed as: $\Delta T = \alpha f^{\frac{1}{2}} r^{-1}$, where ΔT is the critical stress, f is the volume fraction of second particles, r is the average diameter of secondary particles, and α is a constant value. Therefore, the mechanical properties are strongly affected by the size and the amount of the second particles. SEM revealed that the amount of second particles is higher and the size of precipitates is smaller in constraint-aged sample compare with the free-aged samples, which may account for the improvement of the mechanical properties. On the other hand, the water-vapor like bubbles distributing along the grain boundary also play the important role in affecting the compressive properties of constraint-aged Ni–Mn–Ga–Ti alloy. The existence of the bubbles at the grains boundaries effectively hinders the movement of dislocation and the propagation of the crack, which is one of the reasons for the enhancement of the strength. However, with the increasing aging temperature, the benefits resulting from the refinement effect are offset by the coarsened Ni_3Ti precipitates, which results in the decrease in the compressive stress.

To clarify the fracture mechanism and investigate the nucleation and propagation of cracks in constraint-aged Ni–Mn–Ga–Ti alloy, the SEM observations of the fracture surfaces were performed, as shown in Fig. 6. It can be seen that the fracture surface of solution-treated Ni–Mn–Ga–Ti alloys exhibit typical brittle characteristics with an intergranular pattern, and this intergranular pattern becomes weaker after aging treatment, as shown in Fig. 6b and c. In addition, some tearing edges have also been observed, as indicted by the arrow in Fig. 6a. The fracture surfaces of aged $Ni_{53}Mn_{23.5}Ga_{18.5}Ti_5$ alloy exhibits characteristics of ductile fracture, as evidenced by the formation of some small dimples consistent with the literature [25], indicated by the arrows in Fig. 6b. The amount of these dimples increases and the shape changes with the presence of the second particles in the constraint-aged sample, which provides the evidence that more courses needed to be completed and more energy was consumed before fracture.

The mechanism of the ductility improvement in aged Ni–Mn–Ga–Ti is similar to the toughening mechanism of the composite materials. The brittle matrix is connected by the ductile second particles, and the improvement of the ductility is partly provided by the plastic deformation of the ductile second phase introduced by aging treatment. When deformed, the microcracks generated and propagated along the intergranular boundaries. When the original crack meets the second particles, the particles can be plastically deformed. Besides, the crack will stop propagating or directly traverse the second particles while expanding to the boundaries between the matrix and the second phase. All these effects will certainly increase the energy for the crack propagation, thus giving the increase of ductility.

The above results clearly demonstrate that the constraint-aging treatment remarkably affects the phase transformation behavior and can greatly improve the mechanical properties, which can be attributed to the formation and growth of the second particle during aging.

Results and discussion

In this study, the mechanical properties of Ni–Mn–Ga–Ti polycrystalline alloys are improved by introducing a

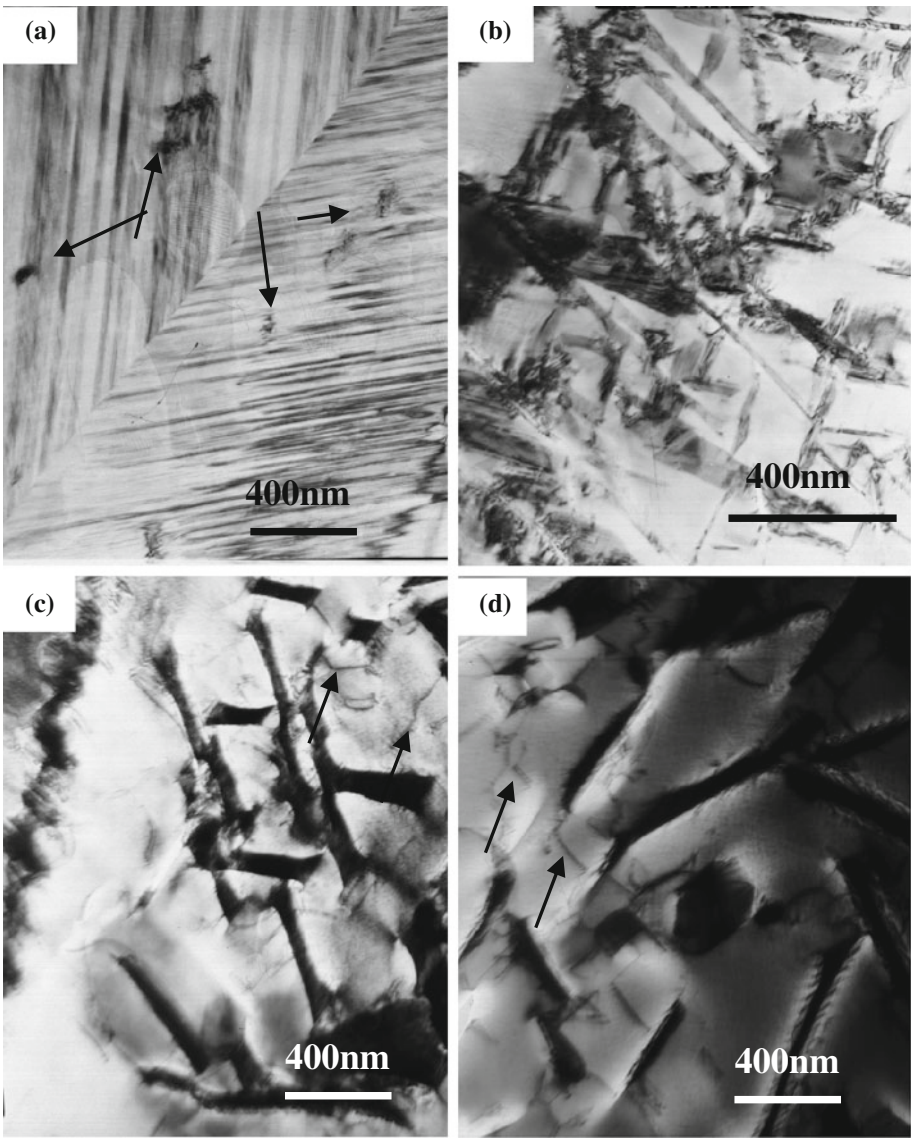

Fig. 5 TEM images of microstructure in the $Ni_{53}Mn_{23.5}Ga_{18.5}Ti_5$ aged at different temperature for 3 h under 2% constant compression strain. **a** $T = 823$ K; **b** $T = 873$ K; **c** $T = 973$ K; and **d** $T = 1073$ K

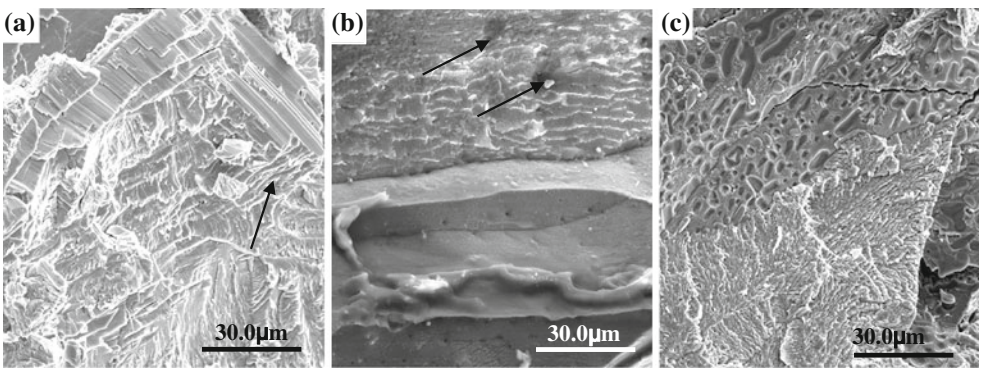

Fig. 6 SEM observations of the fracture surface of $Ni_{53}Mn_{23.5}Ga_{18.5}Ti_5$ alloys under various conditions after compression tests. **a** Solution treated; **b** free aged at 873 K for 3 h; and **c** constraint-aged at 873 K for 3 h

second phase by constraint-aging treatment. On the basis of the studies on martensitic transformation, mechanical properties and microstructure as functions of constraint-aging temperature, the following conclusions are obtained:

(1) The martensitic transformation temperatures first decrease remarkably with the increase of aging temperature, and then increase when the aging temperature exceeds 973 K, which can be attributed to the change of the Ni content in the matrix as well as the strengthening effect by fine Ni_3Ti precipitates.
(2) The constraint aging can promote the nucleation of the second phase. For the constraint-aged Ni–Mn–Ga–Ti alloy, the amount of the Ni-rich precipitates is more, and the size of the second phase particle is smaller in comparison with the free-aged samples. The size of the second particles increase with the increasing constraint-aging temperature.
(3) The compressive stress and ductility can be significantly improved by the constraint-aging treatment. With increasing constraint-aging temperature, the ductility increases while the compressive stress first increases and then decreases, and the maximum compressive stress is about 1400 MPa, which is the highest compressive stress up to date compared with the 400 MPa in solution-treated Ni–Mn–Ga–Ti alloy and about 900 MPa in Ni–Mn–Ga–Ti alloy free-aged at 1073 K for 3 h.
(4) The existence of the Ni-rich second particles plays a key role in improving the compression stress and ductility of Ni–Mn–Ga–Ti alloy.

Acknowledgements This study is supported by Postdoctoral Science Foundation of China (Grant No. 20100481218) and Natural Science Foundation of China (Grant Nos. 50601006, 20973028).

References

1. Ullakko K, Huang JK, Kanter C, Kokorin VV, O'Handley RC (1996) Appl Phys Lett 69:1966
2. Wuttig M, Liu L, Tsuchiya K, James RD (2000) J Appl Phys 87(9):4707
3. O'Handley RC, Murray SJ, Marioni M, Nembach H, Allen SM (1998) J Appl Phys 83(6):3263
4. Mullner P, Chernenko VA, Kostorz G (2004) J Appl Phys 95:1531
5. Hosoda H, Wakashima K, Sugimoto T, Miyazaki S (2002) Mater Trans 43:852
6. Murray SJ, Marioni M, Allen SM, O'Handley RC, Lograsso TA (2000) Appl Phys Lett 77:886
7. Sozinov A, Likhachev AA, Ullakko K (2002) IEEE Trans Magn 38:2814
8. Gao L, Cai W, Liu AL, Zhao LC (2006) J Alloy Compd 425:314
9. Tsuchiya K, Tsutsumi A, Ohtsuka H, Umemoto M (2004) Mater Sci Eng A 378:370
10. Nakanishi N, Mori T, Miura S, Murakami Y, Kachi S (1973) Philos Mag 28:277
11. Khan M, Dubenko I, Stadler S, ALi N (2004) J Phys Condens Matter 16:5259
12. Stadle S, Khan M, Mitchell J, Ali N, Gomes AM, Dubenko I, Takeuchi AY, Guimaraes AP (2006) Appl Phys Lett 88:192511
13. Wang HB, Chen F, Gao ZY, Cai W, Zhao LC (2006) Mater Sci Eng A 438–440:990
14. Cong DY, Wang S, Wang YD, Ren Y, Zuo L, Esling C (2007) Mater Sci Eng A 473:213
15. Glavatskyy I, Glavatska N, Dobrinsky A, Hoffmann J-U, Söderberg O, Hannula S-P (2007) Scripta Mater 56:565
16. Khan M, Dubenko I, Stadler S, Ali N (2005) J Appl Phys 97:10M304-1
17. Dong GF, Cai W, Gao ZY, Sui JH (2008) Scripta Mater 58:647
18. Dong GF, Tan CL, Gao ZY, Feng Y, Cai W, Sui JH (2008) Scripta Mater 59:268
19. Gao ZY, Dong GF, Cai W, Sui JH, Feng Y, Li XH (2009) J Alloy Compd 481:44
20. Dong GF, Gao ZY, Tan CL, Cai W, Sui JH (2010) J Mater Sci 45:5490. doi:10.1007/s10853-010-4606-1
21. Scanchez-Alarcos V, Perez-Landazabal JI, Recarte V, Gomez-polo C, Rodriguez-Velamazan JA (2008) Acta Mater 56:5370
22. Chen XQ, Lu X, Wang DY, Qin ZX (2008) Smart Mater Struct 17:065030
23. Cong DY, Wang S, Wang YD, Ren Y, Zuo L, Esling C (2008) Mater Sci Eng A 473:213
24. Hae-Min Lee, Anthony JK, Rotermund F et al (2009) J Mater Sci 44:3731. doi:10.1007/s10853-009-3498-4
25. Coughlin JP, Williams JJ, Chawla N (2009) J Mater Sci 44:700. doi:10.1007/s10853-008-3188-7